18TH WORLD CONFERENCE ON EARTHQUAKE ENGINEERING
WCEE2024
MILAN

MILAN, ITALY
30TH JUNE - 5TH JULY 2024
www.wcee2024.it

# RAPID POST-EVENT REPAIR COST ASSESSMENT: THE 2023 KAHRAMANMARAŞ EARTHQUAKE SEQUENCE

S. Majdalaweyh[1], A. Jayaprakash[1], S. Dougherty[1], N. Kishi[1] & E. Tasdemir[2]

[1] Karen Clark & Company, Boston, USA, ajayaprakash@karenclarkandco.com

[2] College of Engineering and Technology, American University of the Middle East, Egaila, Kuwait

**Abstract:** *A devastating M7.8 earthquake struck southeastern Türkiye near Pazarcık on February 6th, 2023 resulting in over 50,000 fatalities and damage to over 1.9 million housing units. This earthquake was the largest magnitude event to occur in Türkiye since the 1939 Erzincan M7.8 earthquake. Following this event, we conducted a rapid post-event damage assessment survey covering over 1,200 buildings in four cities. We introduce a novel procedure for expeditiously and systematically collecting and statistically analysing building damage and loss data at a neighborhood level and demonstrate this procedure for damage data collected after the Pazarcık earthquake. The four cities chosen - Antakya, İslahiye, İskenderun, and Dörtyol - represent areas impacted by high and low levels of ground motion intensity. In each surveyed city, two to three neighborhoods spanning between 100-150 buildings were selected. Each building was also assigned characteristics such as year of construction, number of stories, construction type, and occupancy type. Mean repair cost (MRC) was then estimated for each neighborhood using the new procedure. These MRCs can serve as validation points for portfolio level vulnerability functions typically used in catastrophe models, which would enhance the accuracy of catastrophe models, enabling better risk management and preparedness in the region.*

## 1 The Event, Its Impact, and Loss Estimation

In southeastern Türkiye, the African (AF), Arabian (AR), and Anatolian (AN) tectonic plates meet along a series of primarily transform plate boundaries, with translational motion between the AN and AR plates accommodated along the East Anatolian fault zone (Figure 1). In northern Türkiye, the southwest motion of the AN plate is accommodated along the North Anatolian fault zone, which delineates the transform boundary between the AN and Eurasian plates. Earthquakes are common near these strike-slip fault systems, with more than 50 earthquakes of M6.0 or larger since 1900, including 12 earthquakes that were M7.0 or larger.

At 04:17 on 6 February 2023, local time in Türkiye, the Pazarcık M7.8 earthquake occurred near the triple junction of the AF, AR, and AN plates in southeastern Türkiye, approximately 37 km northwest of Gaziantep (Figure 1). It was followed by numerous aftershocks, the largest of which was the Elbistan M7.5 earthquake. Collectively, these events are termed the Kahramanmaraş earthquake sequence. The Pazarcık M7.8 event is attributed to strike-slip faulting at shallow depth within the East Anatolian fault zone. This event is the largest magnitude earthquake to occur in Türkiye since the 1939 Erzincan M7.8 earthquake, though a large-magnitude earthquake (M7.6) struck the region near İzmit in 1999.

Impacts of the Kahramanmaraş earthquake sequence were widespread, affecting eleven provinces comprising 14% of all housing units in Türkiye. The earthquakes caused over 50,000 deaths and far more injuries. The

Ministry of Environment, Urbanization, and Climate Change (MoEUCC) estimated around 1.9 million housing units as at least lightly damaged, of which, over half a million as severely damaged, collapsed, or in urgent need of demolition (Presidential Strategy and Budget Directorate, 2023). Hatay had the highest number of damaged housing units. Kahramanmaraş, where the epicenters of the Pazarcık M7.8 and Elbistan M7.5 earthquakes were located, had the second highest number of housing units damaged, and Malatya, the third. Many commercial buildings also suffered significant damage, including about 8,000 educational buildings and 140 hospitals.

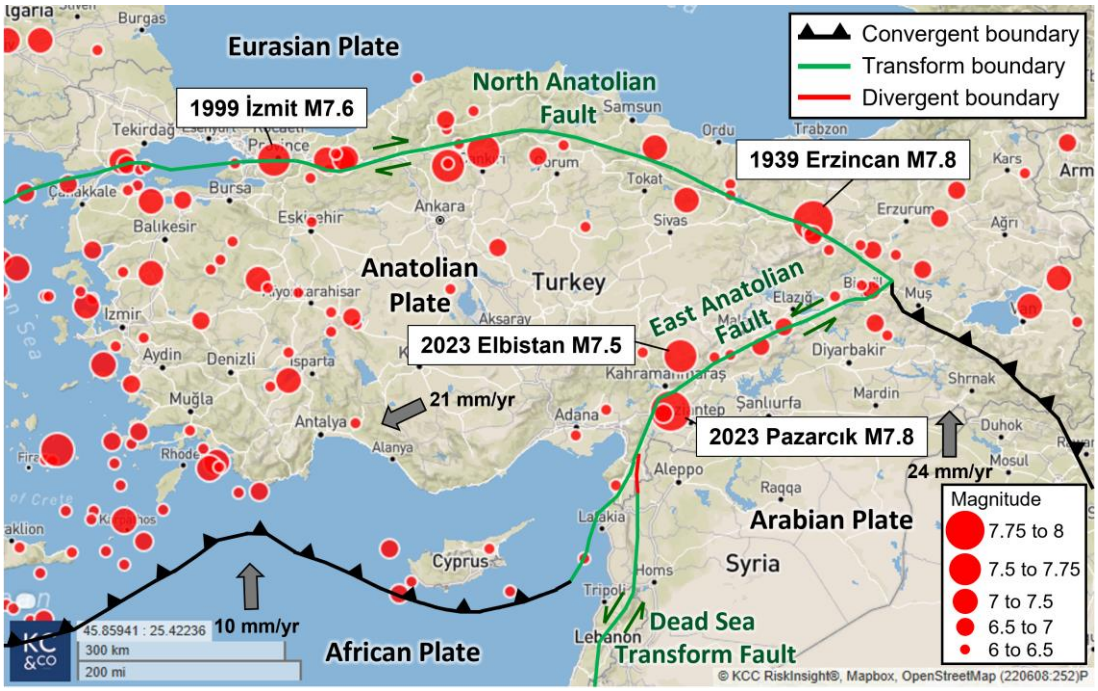


*Figure 1. Tectonic setting and historical seismicity (1900-2023) M6.0 and greater for Türkiye. Relative plate motions indicated by arrows. All earthquake magnitudes given as moment magnitude.*

The World Bank estimated that the Pazarcık M7.8 and Elbistan M7.5 earthquakes caused around TRY 645 billion in direct physical damages in Türkiye, which amounts to around 4% of the country's 2021 Gross Domestic Product (GDP). The total economic losses could be much higher. United States Geological Survey Prompt Assessment of Global Earthquakes for Response (USGS PAGER) estimated a 36% chance that the total economic losses will exceed USD 100 billion or TRY 1.8 trillion.

For residential buildings, Türkiye has a compulsory earthquake insurance program implemented through the Turkish Catastrophe Insurance Pool (TCIP), which was established in 2000. The main objective of this pool is to ensure faster recovery and community resilience after earthquakes. However, there is still a huge protection gap existing in the country. TCIP pays claims for building damage based on its assessment with a maximum coverage limit of TRY 640,000 per policy. However, the cost of reconstruction can be higher than the coverage limit. Additionally, a low percentage of the total number of TCIP-eligible buildings are insured because, typically, the compulsory program can only be enforced for newly purchased homes. Moreover, there is a significant proportion of ineligible buildings, which are buildings in village areas or non-compliant buildings.

The large protection gap is also evidenced by the estimated losses reported to the insurance industry after the Kahramanmaraş earthquake sequence. There are around one million insured residences in the earthquake-affected area with more than TRY 200 billion coverage, based on TCIP's 2021 Annual Report (TCIP, 2021). According to PERILS, an organization that collects insurance market data, the total claims paid as of August 2023 are around TRY 92 billion.

Immediately after the Pazarcık M7.8 and Elbistan M7.5 events, many catastrophe model vendors estimated insured losses near the PERILS-reported numbers, i.e., between TRY 80 – 120 billion. Catastrophe models are computer models that estimate losses for many types of catastrophes, including earthquakes. There are four basic components of a catastrophe model, namely, hazard, exposure, vulnerability, and financial

calculations (Grossi et al., 2005). Earthquake hazards can be characterized by what are referred to as ground motion footprints, which are geospatial representations of the earthquake intensity. USGS ShakeMap is an example of a ground motion footprint. Exposure is a database of geocoded locations of property or other assets exposed to the said hazard. For a building, along with its geographic coordinates, other features are included in the exposure such as its construction type, occupancy type, age, and number of stories. These features determine the relative vulnerability of the property, which is assessed using the vulnerability component. Catastrophe models utilize vulnerability functions for different types of buildings that provide the repair cost for any given intensity. Finally, the financial module applies all the loss terms specific to insurance contracts. Clark (2002) provides details about the origins and applications of catastrophe models.

One of the ways catastrophe models are validated is by ground truthing the models by comparing the results to real damage observations after earthquake events. Post-event damage surveys reveal a lot of information about building performance in the region, relative vulnerability of building types, and general levels of damage for different levels of ground motion intensity. The main objective of this paper is to introduce a novel procedure of systematically collecting and statistically analysing building damage and loss data at a neighborhood level and demonstrating this procedure after the recent earthquakes in Türkiye. A second objective of this paper is to provide results of this study, which will serve as points of validation for catastrophe models.

## 2 Types of Post-event Damage Surveys and Focus on Repair Cost

Post-event damage surveys can broadly be classified into two types: general reconnaissance and statistical survey (Figure 2). Earthquake reconnaissance missions focus on building, infrastructure, or geotechnical specific damage observations. The purposes herein are to learn from site observations about common failure modes, whether any new types of building deficiencies are revealed, or if any changes are warranted in the building codes or enforcement policies. Teams conducting these surveys often carry interests in specific topics such as damage to residences, schools, hospitals, etc. The immediate takeaways from such surveys are qualitative descriptions of building, infrastructure, or ground failure observations.

Statistical surveys are more focused on obtaining a statistical picture of building vulnerability in the area. A larger number of buildings are surveyed with a lower emphasis on specific damage modes and more emphasis on the general level of building damage. The purpose of this type of survey is either to aid recovery planning, as in the case of the survey conducted by the MoEUCC after the Kahramanmaraş earthquake sequence, or for improving or validating loss estimation models by empirically obtaining building fragility or vulnerability functions. The focus of this paper is on this second type of post-event damage survey.

Most studies that fall in the statistical survey type classify the surveyed buildings in a few different bins representing damage states. However, there are no internationally accepted standard descriptions of building damage states (Roeslin et al., 2018); different countries follow their own recommended damage descriptions. For example, the European Macroseismic Scale 1998 (Grünthal, 1998) provides descriptions of different levels of building damage states useful for post-event evaluation across Europe. AeDES (Baggio et al., 2007) provides similar damage states, which are explicitly utilized in Italy. FEMA 306 (Applied Technology Council, 1999) delineates different levels of component damage states and provides guidance for damage evaluation with a focus on building types in the United States. Several authors conducting post-event damage evaluations have also defined damage state descriptions specific to their study.

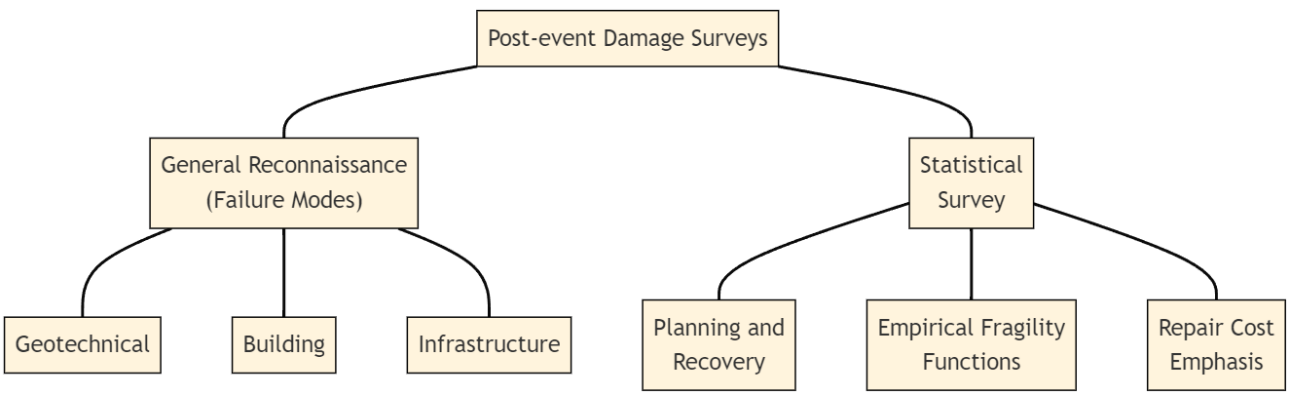


*Figure 2. Illustration of different focus types during post-event damage surveys.*

Dolce and Goretti (2015) used AeDES to perform a post-event survey after the 2009 L'Aquila, Italy M6.3 earthquake and identified the percentage of buildings in each of the physical damage states. Similar damage characterization has been popular after many significant earthquakes, including recent events such as 2017 Puebla, Mexico M7.1 (Roeslin et al., 2018), 2021 Haiti M7.2 (Whitworth et al., 2022), 2023 Pazarcık M7.8 (Presidential Strategy and Budget Directorate, 2023), and many others. The main goal for such characterizations is to enable planning organizations to prioritize resource mobilization based on the damage map of the area. An independent line of inquiry by researchers using similar damage classification data exists for developing empirical fragility functions for different building types. For example, Rosti et al. (2021) derived empirical fragility curves for Italian reinforced concrete (RC) buildings based on damage data from the 1980 Irpinia and 2009 L'Aquila earthquakes. For such studies, it is critical that the damage observations are near seismic stations with recorded ground motions. It is important to note that the damage states used in the aforementioned studies represent physical damage to a building and not any amount of monetary damage.

### 2.1 Monetary Damage or Repair Cost

From the perspective of monetary loss estimation, simply classifying buildings into physical damage states is not sufficient. This is because physical damage states of buildings do not correlate well with repair or replacement cost (Del Vecchio et al., 2020). For validating catastrophe models, which are generally used for estimating insurance loss perspective, repair or replacement cost is of utmost importance. The emphasis here must be on estimation of actual incurred monetary costs from an event, as shown in the bottom-right corner of Figure 2. There are not many studies or procedures that explicitly account for repair cost in a post-event damage survey. De Martino et al. (2017) collected and analysed damage data of residential buildings after the 2009 L'Aquila earthquake by incorporating relevant Actual Repair Costs (ARC) per square foot. For different building components, dividing square footage ARC by the total construction cost per square foot produces the repair cost ratio per component. When all components are combined, it produces the building repair cost ratio.

De Martino et al. (2017) also explored the correlation between repair cost and a damage index defined through physical damage observations. Their results suggest a lack of good correlation between physical damage and repair cost. Even if a building shows moderate physical damage, it does not mean that it would be repaired because the costs could be too high compared to simply rebuilding. For example, after the 2009 L'Aquila earthquake 26% of moderately-to-severely damaged RC buildings were demolished, among them were buildings with seemingly low damage (Polese et al., 2018). Likewise, after the 2010-2011 Canterbury earthquake sequence, 60% of buildings with three or more stories with moderate physical damage in Christchurch were demolished (Gonzalez et al., 2021). Building demolition is not only a function of physical damage, but also other factors such as insurance, owner preference, and building legislation (Marquis et al., 2017). TCIP recently revised its damage assessment methodology to deem buildings that require comprehensive structural interventions as candidates for demolition-and-reconstruction (Akkar et al., 2021).

In this paper, a rapid damage survey procedure termed Neighborhood Level Damage Survey (NLDS), which incorporates the repair cost-to-physical damage relationship, is demonstrated using real residential building damage data after the Kahramanmaraş earthquake sequence. Details of this procedure, including systematic collection of damage data, rigorous analysis, and useful results are discussed in the following sections.

## 3 Neighborhood Level Damage Survey (NLDS)

The Neighborhood Level Damage Survey (NLDS) procedure is designed to quantify site-observed damage data in terms of monetary mean repair cost at the resolution of neighborhoods. A neighborhood is defined as any geographical area that consists of many buildings (100 or more in this study). Steps of the NLDS procedure are as follows.

### 3.1 Neighborhood Selection and Data Collection Format

To demonstrate the rapid damage survey framework, cities from the provinces of Hatay and Gaziantep were selected. Three cities from Hatay (Antakya, İskenderun, and Dörtyol) were selected as candidates because they experienced a range (high, medium, and low, respectively) of ground motion intensities (Figure 3). A fourth city, İslahiye, was selected from the nearby province of Gaziantep which experienced ground motion intensities between that of Antakya and İskenderun.

In each city, two to three neighborhoods were randomly selected to ensure adequate coverage inside the city boundary. Multiple neighborhoods within the same city are crucial to eliminate any spurious damage patterns that emerge from the data. For example, we cannot generalize any damage pattern if it is observed only within one neighborhood of a city. While three neighborhoods may be adequate, many more are desirable. Figure 4 illustrates the location of three neighborhoods selected from within the city of Antakya. An aerial view of a sample of the assessed buildings in one of these neighborhoods is also shown.

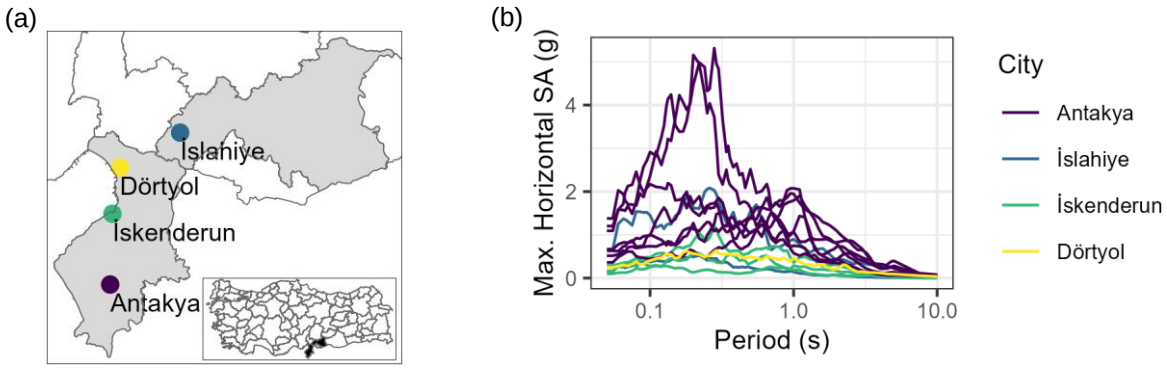


*Figure 3. (a) Selected cities and (b) the recorded acceleration response spectra at different stations across Antakya, İslahiye, İskenderun, and Dörtyol. Spectra are color-coded by city.*


*Figure 4. Selected neighborhoods in Antakya (blue stars) and a sample of assessed buildings (gray circles).*

An assessment of each building was made regarding their structural and non-structural damage. From all four cities, the total number of inspected buildings is 1,231. In addition to damage, other key attributes were also recorded for each building, which included:

1. Building height (Low-, Mid-, or High-rise).
2. Building age (Pre-2000 or Post-2000).
3. Occupancy type (Residential, Commercial, or Industrial).
4. Construction material (Reinforced Concrete or Masonry).

Of the 1,231 buildings surveyed, 1,137 were reinforced concrete (RC) residential buildings. The distribution of low- (< 4 stories), mid- (4-8 stories), and high-rise (> 8 stories) residential buildings within different locations is shown in Figure 5a. Low-rise and mid-rise buildings predominate the surveyed inventory, and there were only a handful of high-rise buildings. For building age, it was decided to classify the buildings as either built before or after 2000, as shown in Figure 5b. Note that seismic building codes in Türkiye underwent substantial revisions following the 1999 İzmit and Düzce earthquakes. To ensure building ductility, building codes introduced stringent regulations, such as strong column-weak beam design and more intricate reinforcement detailing. Consequently, buildings constructed after 2000 should be less vulnerable to earthquakes.

### 3.2 Damage Assessment

In the rapid post-event assessment, building damage observations are typically limited to the exterior of the building. The interior damage is subsequently inferred from exterior damage in the data post-processing phase

of the procedure, discussed later. Damage assessment in this study can therefore be classified into two phases: exterior damage assessment and interior damage assessment.

*Exterior Damage Assessment Phase*

Exterior assessment entails documenting damage to exterior structural (S) and exterior non-structural (NS) components. The exterior structural components are the load-bearing components such as beams, shear walls, and columns. The exterior non-structural components include infill walls, wall sidings or cladding, windows, doors, and roofs. For each surveyed building, exterior structural and non-structural components were assigned an appropriate damage state based on visual inspection. These damage states (DS) are categorized on a scale ranging from $DS1_S$ to $DS5_S$ for exterior structural and from $DS1_{NS}$ to $DS5_{NS}$ for exterior non-structural components, as detailed in Table 1 and Table 2, respectively. The damage descriptions are based on those provided by Rossetto and Elnashai (2003), adjusted to include damage modes observed in Turkish building stock. The severity of observed damage is characterized by visible cues of performance degradation, such as cracks, deflections, component separations, concrete spalling, and buckling.

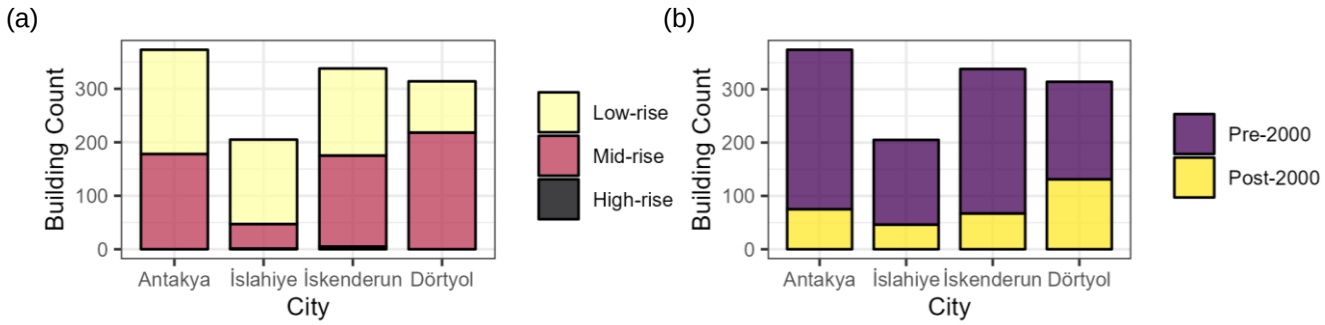


*Figure 5. Distribution of (a) building height and (b) year built in different cities.*

*Table 1. Damage state descriptions for exterior structural components*

| Damage States | Description |
|---|---|
| **$DS1_S$** | No structural damage. Fine cracks in plaster. |
| **$DS2_S$** | Start of structural damage. Small cracking in some beams, columns, or shear walls. |
| **$DS3_S$** | Flexural and/or shear cracking in beams, columns, or shear walls. Start of concrete spalling in some members. |
| **$DS4_S$** | Large flexural cracking, concrete spalling in many members, loss of bond at joints and lap-splices, rebar pull-out or buckling, broken ties, and column shear failure. |
| **$DS5_S$** | Partial or complete building collapse. |

*Table 2. Damage state descriptions for exterior non-structural components*

| Damage States | Description |
|---|---|
| **$DS1_{NS}$** | Fine cracks in plaster partitions/infills. Flaking of paint and plaster. |
| **$DS2_{NS}$** | Cracking initiates from corners of openings. Diagonal cracking of walls. Limited crushing of bricks. |
| **$DS3_{NS}$** | Increased diagonal cracking and spalling at wall corners. Partial failure of some infills/partitions. |
| **$DS4_{NS}$** | Partial failure of many infills/partitions. Extensive damage to openings. |
| **$DS5_{NS}$** | Partial or complete collapse. |

Figure 6 shows examples of typical mid-rise RC buildings photographed during the survey and their corresponding damage classification based on the criteria listed above. The building in Figure 6a did not have any exterior structural damage but fine cracks in the plaster of infill walls ($DS1_S$ and $DS1_{NS}$). The building in Figure 6b had small cracking in beams and columns and initiated cracks from corners of openings in addition

to diagonal cracking in infill walls ($DS2_S$ and $DS2_{NS}$). Some structural members in the building in Figure 6c had concrete spalling in addition to out-of-plane failure of exterior infill walls ($DS3_S$ and $DS3_{NS}$). And the building in Figure 6d had extensive collapse of exterior infill walls and first floor column concrete core crushing and bar buckling that led to a soft-story collapse behavior ($DS4_S$ and $DS4_{NS}$). Note that these photos are only examples, and the procedure does not restrict the S and NS damage states to always be the same number.

(a) (b) (c) (d)

*Figure* 6. *Examples of mid-rise Reinforced Concrete (RC) building damage observations from all damage states: (a) $DS1_S$ and $DS1_{NS}$, (b) $DS2_S$ and $DS2_{NS}$, (c) $DS3_S$ and $DS3_{NS}$, (d) $DS4_S$ and $DS4_{NS}$.*

Figure 7a presents the frequency of the building exterior structural and non-structural damage states in the complete set of surveyed buildings. About 600 (~50%) buildings experienced slight damage of DS1 for both structural and non-structural components, with 81% of these buildings in İskenderun and Dörtyol, which experienced lower ground motion intensities. A total of 160 buildings (13%) in the dataset completely collapsed, of which 83 were in Antakya. Ninety percent of these collapsed buildings were built before 2000. Figure 7b shows the joint probability mass of structural and non-structural damage states in the collected data. Note how structural damage state DS1 can result in any of the non-structural damage states, whereas higher structural damage states tend to result in non-structural damage states at or above the corresponding DS number. At structural damage states DS3 or DS4, it is virtually certain that the non-structural damage state would be DS4.

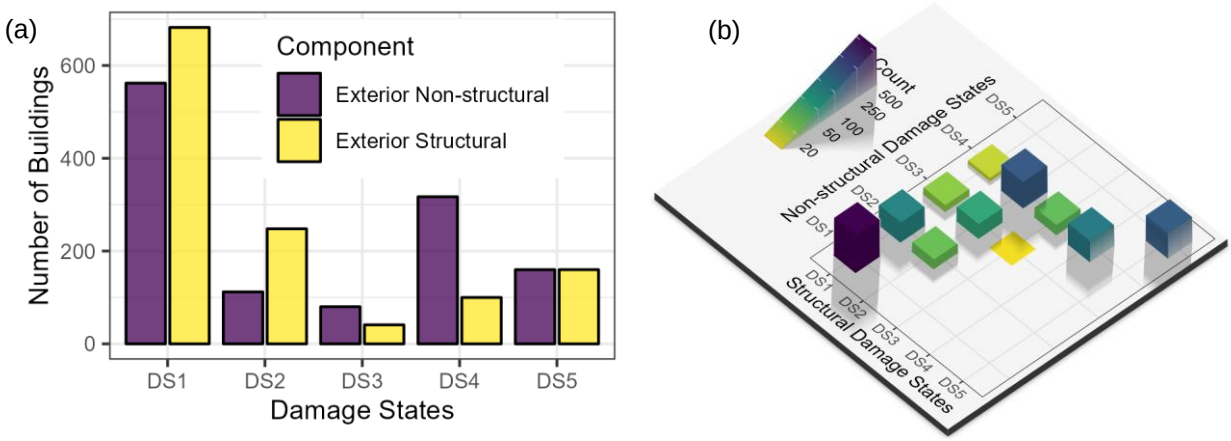


*Figure 7. (a) Frequency of the different damage states in the surveyed area. (b) Joint probability mass of structural and non-structural damage states.*

*Interior Damage Assessment Phase*

The interior of a building, which is not directly observable, is divided into three different components: (1) interior structural components (IS), which are the internal load-bearing components, (2) interior non-structural components (INS), which are partition walls and doors inside the building, and (3) building interior and finishes (BIF), which include floor covering, plastering and painting, plumbing, and mechanical and electrical components. The interior components' damage states are inferred from damage states of exterior components using engineering intuition and the general damage correlation observed between exterior structural and non-structural components, as shown in Figure 7b. Engineering intuitions are calibrated to the Kahramanmaraş earthquake sequence by visiting the interiors of a few buildings in each neighborhood. Figure 8 illustrates the overall procedure.

Under earthquake shaking, it is assumed that the exterior and interior structural components perform the same. Although exterior structural members may be subjected to additional stress due to torsional effects, it is ignored here. The interior non-structural component damage state is a function of exterior non-structural damage and interior structural damage. This follows the idea that non-structural component damage could be classified into drift sensitive and acceleration sensitive. Structural damage acts as a proxy for drift demand. While there is no one-to-one visually observable proxy for the acceleration demand, the general level of exterior non-structural damage, which is a function of both drift and acceleration demand, is assumed to be a sufficient proxy.

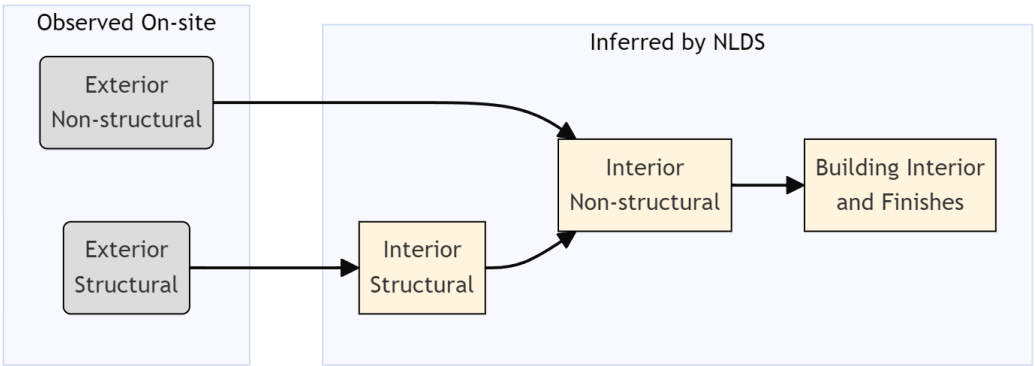


*Figure 8. Relationship between observed and inferred damage states.*

Figure 9 shows the proposed matrix to define the interior non-structural components damage state. For example, if the observed exterior structural damage state is $DS2_S$ (Table 1), the interior structural damage state is $DS2_{IS}$, which will have the same description as $DS2_S$. If then, the observed exterior non-structural damage is $DS3_{NS}$ (Table 2), the interior non-structural damage will be inferred to be $DS3_{INS}$. Here, $DS3_{INS}$ has the same description as $DS3_{NS}$.

The damage state of the last component, BIF, is assumed to be the same as the interior non-structural component because, in Türkiye, plumbing and electrical equipment are commonly incorporated within hollow bricks used as partition walls. It follows that damage to interior non-structural components is correlated to the damage to BIF.

| **Determination of Interior Non-Structural Components Damage State** | | **Exterior Non-Structural Components** | | | | |
|---|---|---|---|---|---|---|
| | | **$DS1_{NS}$** | **$DS2_{NS}$** | **$DS3_{NS}$** | **$DS4_{NS}$** | **$DS5_{NS}$** |
| **Interior Structural Components** | **$DS1_{IS}$** | $DS1_{INS}$ | $DS2_{INS}$ | $DS3_{INS}$ | $DS4_{INS}$ | $DS5_{INS}$ |
| | **$DS2_{IS}$** | $DS2_{INS}$ | $DS2_{INS}$ | $DS3_{INS}$ | $DS4_{INS}$ | $DS5_{INS}$ |
| | **$DS3_{IS}$** | $DS3_{INS}$ | $DS3_{INS}$ | $DS4_{INS}$ | $DS4_{INS}$ | $DS5_{INS}$ |
| | **$DS4_{IS}$** | $DS4_{INS}$ | $DS4_{INS}$ | $DS4_{INS}$ | $DS4_{INS}$ | $DS5_{INS}$ |
| | **$DS5_{IS}$** | $DS5_{INS}$ | $DS5_{INS}$ | $DS5_{INS}$ | $DS5_{INS}$ | $DS5_{INS}$ |

*Figure 9. Determination matrix of interior non-structural (INS) components damage state based on NS and IS damage states.*

### 3.3 Component Repair Costs

Component Repair Cost Ratio (CRCR) is defined here as the ratio of the repair cost of a component to its total replacement cost. The CRCR is represented by a lognormal distribution for each damage state (Table 3), whose parameters were determined by appropriately modifying those provided by Del Vecchio et al. (2020). This modification was necessary because 1) the repair costs in Del Vecchio et al. (2020) pertain to Italian buildings after the 2009 L'Aquila earthquake (adjustments for Türkiye were made based on consultations with Turkish engineers), and 2) the damage state definitions for this study and Del Vecchio et al. (2020) are slightly different. For example, DS4 in Del Vecchio et al. (2020) is categorically closer to DS3 in this study for the structural component. Akkar et al. (2021) and De Martino et al. (2017) also provide similar guidance on the repair cost distribution.

Table 3 shows the values of mean and dispersion parameters of the lognormal distribution. Note that DS5 does not have a distribution of repair cost since this is a collapse damage state and it is assumed that the building will be replaced, meaning 100% CRCR for structural and non-structural components. Figure 10 shows the corresponding CRCR probability density functions for each damage state for both structural and non-structural components. The physical damage states of all five building components (S, NS, IS, INS, and BIF) were mapped to the appropriate CRCR distribution for all 1,231 buildings in the dataset.

*Table 3. Component repair cost ratio (CRCR) for all components and damage states.*

| **Components** | **Mean (dispersion) parameters of lognormal distribution** | | | | |
|---|---|---|---|---|---|
| | **DS1** | **DS2** | **DS3** | **DS4** | **DS5** |
| **S and IS** | -7.25 (2.59) | -2.45 (0.33) | -1.20 (0.42) | -0.26 (0.16) | - |
| **NS, INS, and BIF** | -6.91 (2.8) | -1.61 (0.42) | -0.57 (0.21) | -0.11 (0.07) | - |

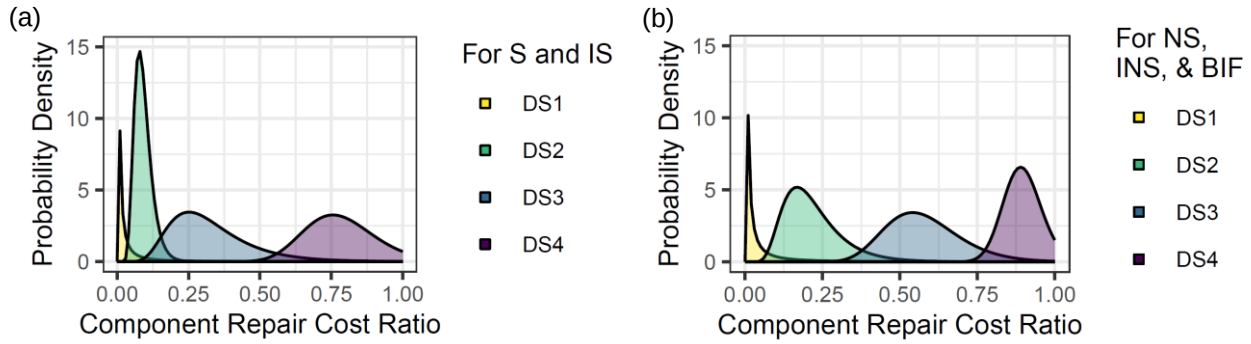


*Figure 10. Lognormal functions of the repair cost ratio of DS1 to DS4 of components (a) S and IS and (b) NS, INS, and BIF.*

### 3.4 Simulation of Mean Repair Cost (MRC) at Building and Neighborhood Levels

N number of realizations of the CRCR for each component is obtained by randomly sampling from the CRCR distributions. To obtain the building level repair cost distribution, mean (MRC), and standard deviation (SD), the next step is to combine the simulated component level cost ratios. This is achieved by performing a weighted average calculation for each simulation, where the weights of the individual components are their respective cost in proportion to the total value of the building. This weight is termed the exposure contribution factor or simply exposure factor. Figure 11 illustrates this process and provides the exposure factors used in this study. The exposure factors are estimated based on typical RC building cost breakdown in Türkiye (Atmaca, 2016). Note that these factors would tend to be different for different building types and buildings in different regions. Therefore, when implementing NLDS for future studies, these will have to be re-assumed. However, a sensitivity analysis showed that the results are not too sensitive to the exposure factors.

A convergence study was conducted to find the optimal number of simulations required for convergence of building MRC. Different values of N equal to 10, 100, 1000, 5,000, and 100,000 simulations were tried. It was found that a relatively modest sample size of 5,000 simulations was sufficient. After obtaining the building level MRC and SD for all 1,231 buildings, the values were aggregated by different variables such as neighborhoods, building height, and year built, as discussed next.

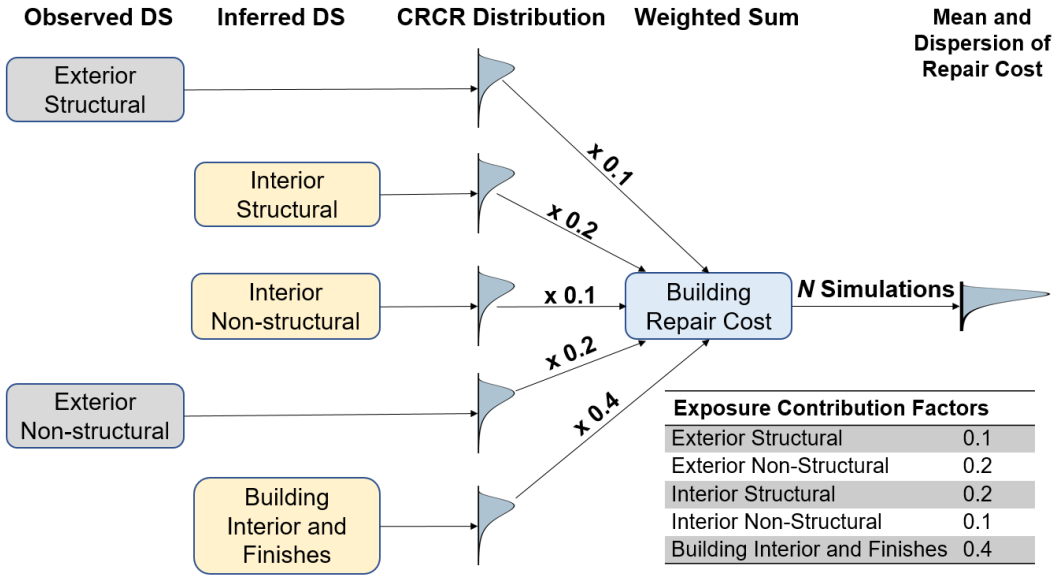


*Figure 11. Illustration of the calculation process for the mean repair cost (MRC) of each building.*

## 4 Results and Discussion

### 4.1 Mean Repair Costs by Neighborhoods

Results after aggregating the building level repair cost distribution for every surveyed neighborhood are as shown in Figure 12. Neighborhoods are classified into their corresponding cities. The color bars show the MRC and the error bars indicate the uncertainty (2 standard deviations) of the repair cost distribution. Note that the uncertainty of high MRCs is much smaller than low MRCs when implementing this procedure. This is also more reflective of reality because at extremely high damage levels, it is almost assured that buildings will be demolished. However, at low to moderate levels of damage, there is larger uncertainty in repair cost (Marquis et al., 2017).

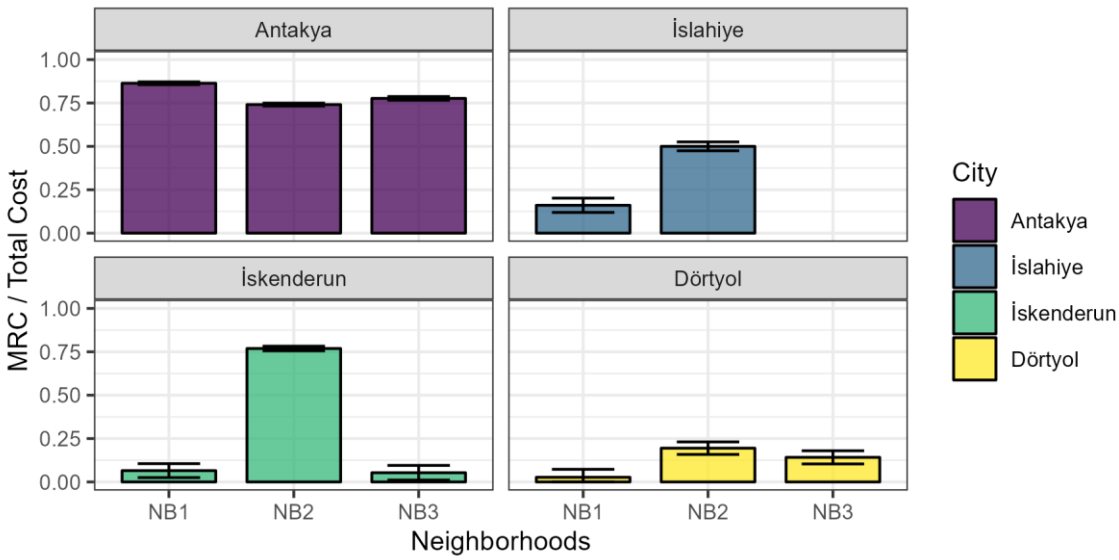


*Figure 12. Estimated mean repair costs (MRC) as a fraction of total cost for all surveyed neighborhoods.*

As expected, cities that generally experienced higher ground motions had higher MRC. All three neighborhoods in Antakya are estimated to have incurred high monetary losses that amount to more than 70% of the total cost of these neighborhoods. In İslahiye, the two neighborhoods surveyed show MRC of 16% and 50%. By surveying an additional neighborhood in İslahiye, a clearer picture of the general level of losses in the city could be obtained. The authors recommend always selecting 3 or more neighborhoods when applying

the NLDS procedure. Dörtyol and İskenderun overall suffered lower losses, except for neighborhood 2 (NB2) in İskenderun.

NB2 in İskenderun shows significantly higher losses than the other two neighborhoods in the city. This is because NB2 consists almost entirely of mid-rise buildings (94 out of 100), while most buildings in NB1 and NB3 are low-rise. It has been observed for the Kahramanmaraş earthquake sequence that mid-rise buildings suffered more damage than low-rise buildings within a given area.

### 4.2 Mean Repair Costs by Building Height and Year Built

When the estimated MRCs are aggregated based on the classification of low-rise and mid-rise buildings, a clear pattern can be observed in all cities. The mid-rise buildings show significantly higher MRCs than low-rise buildings, especially in areas subjected to lower ground motion (GM) intensities. Results from Antakya (high GM) and İskenderun (low GM) are shown in Figure 13a. In both cities, loss to mid-rise buildings was higher than that of low-rise, which is also the case in İslahiye and Dörtyol. Further study is required to reveal the potential reason(s) for this observation, which is beyond the scope of this paper.

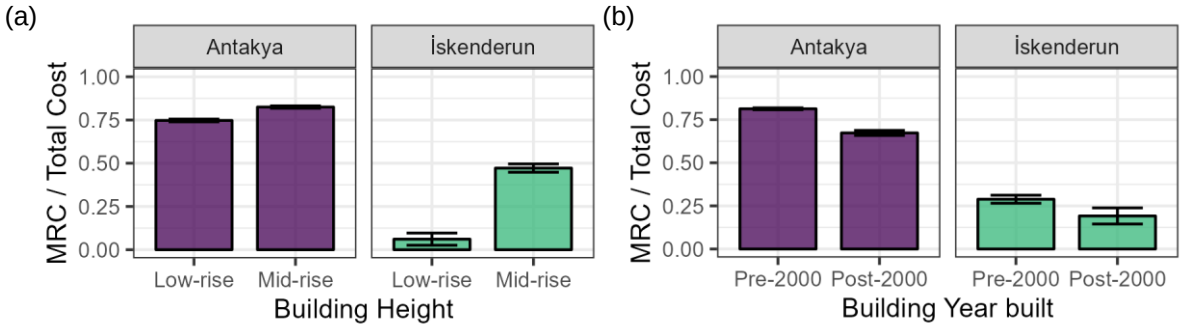


*Figure 13. Estimated mean repair costs (MRC) as a fraction of total cost classified by (a) building height, and (b) building year built.*

It is well known that after the 1999 İzmit earthquake in Türkiye, the building code enforcement became stricter, which generally manifested in the form of better designed buildings after 2000. In general, the loss to pre-2000 buildings was higher in this study than the post-2000 buildings. However, the difference was not as significant as one might have expected, as seen in Figure 13b. This may also lead back to how badly the mid-rise buildings performed. A significant proportion of the post-2000 inventory are mid-rise buildings, which seems to have contributed to a higher MRC.

To further isolate the impact of only the year built era, the data must be subdivided into the same neighborhood and height class. Upon doing this, only one neighborhood in Antakya remains with a significant number of buildings (96). When all mid-rise buildings are reviewed for this neighborhood, pre-2000 buildings (49) have a MRC of 97% and post-2000 buildings (47) have a MRC of 75%. Therefore, at least in this neighborhood, the post-2000 buildings performed better than pre-2000. Moreover, recall that over 90% of all collapsed buildings in the survey were pre-2000. Effectively, it can be surmised that post-2000 buildings have been successful in reducing the likelihood of building collapse, but not as successful in reducing loss likelihood. This observation is good for life safety, but from the perspective of resilience and rebuilding, there is still room for significant improvements.

## 5 Conclusions

In addition to understanding the level of physical damage after earthquakes, there must also be a focus on estimating the total repair cost because there is minimal correlation between the two based on observations from recent events. In this regard, the outcomes of the NLDS procedure, introduced in this paper, hold importance for both the reconstruction phase and considerations related to earthquake insurance pay-outs.

Physical damage data from 11 neighborhoods across 4 cities were collected and analysed using the NLDS procedure to estimate the mean repair costs (MRCs) of these neighborhoods as a fraction of the total replacement cost. These MRCs serve as potential validation points for earthquake catastrophe models of this region. Additionally, data collected as part of this study contributes significantly to the scientific enhancement of building vulnerability assessments for existing structures in southeastern Türkiye.

## 6 References


Akkar, S., Ilki, A., Goksu, C. and Erdik, M. (2021). *Advances In Assessment and Modeling of Earthquake Loss* (p. 308). Springer Nature

Applied Technology Council. (1999). *Evaluation of Earthquake Damaged Concrete and Masonry Wall Buildings: Basic Procedures Manual (FEMA 306), Vol.43,* California.

Atmaca, A. (2016). Life-Cycle Assessment and Cost Analysis of Residential Buildings in South East of Türkiye: Part 2—A Case Study. *The International Journal of Life Cycle Assessment*, 21: 925-942.

Baggio, C., Bernardini, A., Colozza, R., Corazza, L., Della Bella, M., Di Pasquale, G., Dolce, M., Goretti, A., Martinelli, A., Orsini, G. and Papa, F. (2007). Field Manual for Post-Earthquake Damage and Safety Assessment and Short Term Countermeasures (AeDES). *European Commission—Joint Research Centre—Institute for the Protection and Security of the Citizen*, EUR, 22868.

Clark, K.M. (2002). The Use of Computer Modeling in Estimating and Managing Future Catastrophe Losses. *The Geneva Papers on Risk and Insurance*, 27:181–195.

De Martino, G., Di Ludovico, M., Prota, A., Moroni, C., Manfredi, G. and Dolce, M. (2017). Estimation of Repair Costs for RC And Masonry Residential Buildings Based on Damage Data Collected by Post-Earthquake Visual Inspection. *Bulletin of Earthquake Engineering*, 15:1681-1706.

Del Vecchio, C., Ludovico, M.D. and Prota, A. (2020). Repair Costs of Reinforced Concrete Building Components: From Actual Data Analysis to Calibrated Consequence Functions. *Earthquake Spectra*, *36*(1):353-377.

Dolce, M., Goretti, A. (2015). Building Damage Assessment after the 2009 Abruzzi Earthquake. *Bulletin Earthquake Eng*ineering, 13:2241–2264. https://doi.org/10.1007/s10518-015-9723-4

Gonzalez, R.E., Stephens, M.T., Toma, C., Elwood, K.J. and Dowdell, D. (2021). Post-Earthquake Demolition in Christchurch, New Zealand: A Case-Study Towards Incorporating Environmental Impacts in Demolition Decisions. *Advances in Assessment and Modeling of Earthquake Loss*, 47-64.

Grossi, P., Kunreuther, H., Windeler, D. (2005). An Introduction to Catastrophe Models and Insurance, in: Grossi, Partricia, Kunreuther, H. (Eds.), *Catastrophe Modeling: A New Approach to Managing Risk, Catastrophe Modeling*. Boston: Springer, 23–42. https://doi.org/10.1007/0-387-23129-3_2

Grünthal, G. (1998). *European Macroseismic Scale 1998*. European Seismological Commission (ESC).

Polese, M., Di Ludovico, M. and Prota, A. (2018). Post-earthquake reconstruction: A study on the factors influencing demolition decisions after 2009 L'Aquila earthquake. *Soil Dynamics and Earthquake Engineering*, *105*:139-149.

Presidential Strategy and Budget Directorate. (2023). 2023 Kahramanmaraş and Hatay Earthquakes Report (Post-Earthquake Assessment). https://www.sbb.gov.tr/wp-content/uploads/2023/03/2023-Kahramanmaras-ve-Hatay-Depremleri-Raporu.pdf (Last accessed in October 2023).

Marquis, F., Kim, J.J., Elwood, K.J. and Chang, S.E. (2017). Understanding Post-Earthquake Decisions on Multi-Storey Concrete Buildings in Christchurch, New Zealand. *Bulletin of Earthquake Engineering*, *15*:731-758.

Roeslin, S., Ma, Q.T. and García, H.J. (2018). Damage Assessment on Buildings Following the 19th September 2017 Puebla, Mexico Earthquake. *Frontiers in Built Environment*, 4:72.

Rossetto, T. and Elnashai, A. (2003). Derivation Of Vulnerability Functions for European-Type RC Structures Based on Observational Data. *Engineering structures*, *25*(10):1241-1263.

Rosti, A., Del Gaudio, C., Rota, M., Ricci, P., Di Ludovico, M., Penna, A., Verderame, G.M. (2021). Empirical Fragility Curves for Italian Residential RC Buildings. *Bulletin Earthquake Eng*ineering, 19:3165–3183. https://doi.org/10.1007/s10518-020-00971-4

TCIP, 2021. *2021 Annual Report Turkish Natural Catastrophe Insurance Pool.* (https://www.dask.gov.tr/en/annual-reports)

Whitworth, M.R., Giardina, G., Penney, C., Di Sarno, L., Adams, K., Kijewski-Correa, T., Black, J., Foroughnia, F., Macchiarulo, V., Milillo, P. and Ojaghi, M. (2022). Lessons for Remote Post-Earthquake Reconnaissance from the 14 August 2021 Haiti Earthquake. *Frontiers in Built Environment*, 8.